International Information and Engineering Technology Association
Advancing the World of Information and Engineering

International Journal of Heat and Technology
Vol. 36, No. 3, September, 2018, pp. 773-782
Journal homepage: http://iieta.org/Journals/IJHT

Application GMDH artificial neural network for modeling of Al_2O_3/water and Al_2O_3/Ethylene glycol thermal conductivity

Mohammad H. Ahmadi[1*], Fatemeh Hajizadeh[2], Mohammad Rahimzadeh[3], Mohammad B. Shafii[4], Ali J. Chamkha[5,6], Giulio Lorenzini[7], Roghayeh Ghasempour[2]

[1] Faculty of Mechanical Engineering, Shahrood University of Technology, Shahrood, Iran
[2] Faculty of New Sciences and Technologies, University of Tehran, Tehran 1961733114, Iran
[3] Department of Mechanical Engineering, Golestan University, Gorgan, Iran
[4] Mechanical Engineering, Sharif University of Technology, Tehran 11365-11155, Iran
[5] Mech Eng Dept, Endow. Energy and Env., Prince M B Fahd Univ, Al-Khobar 31952, Saudi Arabia
[6] RAK Res., American Univ of Ras Al Khaimah, P.O. Box 10021, United Arab Emirates
[7] Università degli Studi di Parma, Dipartimento di Ingegneria e Architettura, Parma 43124, Italy

Corresponding Author Email: mohammadhosein.ahmadi@gmail.com

https://doi.org/10.18280/ijht.360301

Received: 19 Febraury 2018
Accepted: 2 June 2018

Keywords:
nanofluid, thermal conductivity, GMDH, artificial

ABSTRACT

Thermal conductivity of nanofluids depends on several parameters including temperature, concentration, and size of nanoparticles. Most of the proposed models utilized concentration and temperature as influential factors in their modeling. In this study, group method of data handling (GMDH) artificial neural networks is applied in order to model the dependency of thermal conductivity on the mentioned factors. Firstly, temperature and concentration considered as inputs and a model is represented. Afterwards, the size of nanoparticles is added to the input variables and the results are compared. Based on obtained results, GMDH is an appropriate method to predict thermal conductivity of the nanofluids. In addition, it is necessary to consider size of nanoparticles in order to have a more precise model.

1. INTRODUCTION

Nanotechnology utilization developed in recent years due to their ability to enhance efficiency of energy systems and decrease the size of tools. By applying nanotechnology it is possible to obtain materials with more favorable properties such as mechanical strength, electrical conductivity, thermal conductivity and etc. [1–3]. By applying nanotechnology, the nanofluids are obtained which can be very appropriate for various purposes, especially in heat transfer and thermal processes [4–9].

Nanofluids are prepared by dispersion of particles with nano scale dimension in a base fluid [10–13]. Nanofluids are widely used in heat transfer applications due to their higher thermal conductivity compared with the base fluids [14-15]. Improvement in thermal conductivity of nanofluids is attributed to high surface/volume ratio of nano particles [10, 16]. Several studies have focused on utilization of nanofluids for heat transfer applications [17–20]. Using nannofluids can significantly enhances heat transfer in comparison with pure fluids. Improvement in thermal performances is mainly attributed to higher thermal conductivity of nanofluids in comparison with the base fluid [21].

Rashidi et al. [22] used CuO, Al_2O_3, TiO_2 nano particles in turbine oil to investigate the effect of adding the mentioned nano particles on heat transfer. Results revealed that using the nano particles led to enhancement in heat transfer coefficient. Tabari et al. [23] conducted a study on application of multiwalled carbon nano tubes (MWCNTs)/water in a heat exchanger. Obtained results indicated that using the nanofluid enhance convective heat transfer compared with using the base fluid. In addition to convective heat transfer, applying nanofluids can enhance boiling heat transfer [24-25]. Minakov et al. [26] applied various nano particles including silicon, aluminum, iron oxide and diamond in distilled water and compared boiling heat transfer on cylindrical heater. Results showed that using nanofluids can enhance critical heat flux which was mainly attributed to deposition of nano particles on the surface of the heater. Dadjoo et al. [27] compared pool boiling of SiO_2/ water and water on a flat plate heater. Obtained data revealed that the boiling heat transfer coefficient improved by using nanofluid; however, there was an optimal concentration for improvement in heat transfer.

Nano particles dispersion in a base fluid change its thermophysical specifications [28–33]. Changes in thermophysical properties of nanofluids depend on several factors including size and shape of nano particles, their concentration, and temperature of the nanofluid [34–40]. Among various thermphyiscal properties, thermal conductivity and dynamic viscosity play more important role in thermal behavior of the nanofluids [41]. Several studies have concentrated on the effect of adding nano particles on dynamic viscosity and thermal conductivity of nanofluids [42-46].

Since the cost of experimental research is high in some cases, predicting the thermal conductivity of the nanofluid before testing will reduce the cost and time and provide a detailed experimental design. Hence, in recent years, the prediction of thermal properties of nanofluid with different mathematical methods has been carried out. Nadooshan et al

[47] experimentally measured viscosity of $SiO_2 - MWCNTs$ / 10W40 engine oil and applied artificial neural network in order to predict the viscosity. In the proposed model, shear rate, temperature and concentration solid phase were considered as input variable for the model. Experimental results indicated that the r elative viscosity increased by increasing the concentration of solid phase. The proposed model had good agreement with experimental data and its R-squared value was 0.9948. Alirezaie [48] et al experimentally investigated the effects of concentration, temperature and shear rate on the dynamic viscosity of MWCNT (COOH-Functionalized)/MgO- engine oil. Results showed that dynamic viscosity increased by solid volume concentration increment and decreased by temperature increase. In addition, a correlation was proposed and compared with artificial neural network model to predict the viscosity. Based on the results, artificial neural network showed higher accuracy in modeling. In another study, three artificial neural network approaches including Genetic Algorithm-Radial Basis Function Neural Networks (GA-RBF), Least Square Support Vector Machine (LS-SVM) and Gene Expression Programming (GEP) were utilized to predict dynamic viscosity of TiO_2 / SAE 50 nanofluid [49]. The results of the models indicated that GA-RBF method had the best accuracy among the applied approaches.

In addition to models proposed for predicting dynamic viscosity of nanofluids, there are some studies which have focused on thermal conductivity of nanofluids [50]. Hemmeat Esfe et al. [51] experimentally assessed ZnO-MWCNT/EG-water thermal conductivity and utilized artificial neural network to model the thermal conductivity. The effects of temperature and concentration were considered in this study. The volume fraction of solid was in the range of 0.02 to 1% and the temperature varied between 30 and 50 ℃ Results indicated that the thermal conductivity ratio of nanofluids increased by increasing the temperature and volume fraction of solid phase. Afrand et al. [52] proposed a correlation by using curve fitting and design an artificial neural network to predict thermal conductivity of MgO/water nanofluids. The input variables were temperature and nano particles concentration in the base fluid. Comparison between the outputs of neural network model and the proposed correlation revealed that the accuracy of the artificial neural network model was higher than the empirical correlation.

Based on literature review, artificial neural network modeling is an appropriate tool to model and predict thermal conductivity of nanofluids. Most of the conducted studies have considered temperature and concentration as influential parameters and input variables [53–57]; however, the size of nano particles affect thermal conductivity of nanofluids. In this study, group method of data handling (GMDH) artificial neural network is applied in order to model thermal conductivity ratio of Al_2O_3 /water and Al_2O_3 /EG because Al_2O_3 nanofluid is a usual nanofluid. The applied algorithm in this study is novel and powerful for modeling to determine the relationship of Al_2O_3 nanoparticles concentration, size and fluid temperature to nanofluid thermal conductivity of water and ethylene glycol as a coolant fluid.

2. METHOD

GMDH artificial neural network is an accurate and powerful predictive approach which is applicable for modeling of engineering systems and recognition of patterns. GMDH is a self-orgnizing network and one-directional. There are various layers in these types of networks and the neurons contain 1 output and 2 inputs as illustrated in figure 1. The neurons have one bias and 5 weights.

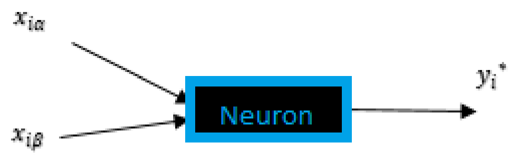

Figure 1. Structure of neuron in GMDH

In order to correlate inputs and output in each layer, Volterra functional series are used. Details about this algorithm and working principles are presented in ref [56].

3. RESULTS AND DISCUSSION

T In order to model the thermal conductivity ratio of the nanofluids, GMDH method is applied. In the first step, the thermal conductivity ratio of the nanofluids is considered as a function of temperature and volumetric concentrations. Afterwards, the size of nano particles added to the input variables and the results are compared with each other. Ranges of each parameter are represented in tables 1 & 2.

Table 1. Ranges of parameters for Al_2O_3/water nanofluid

Parameter	Range
Temperature (℃)	10-70
Volumetric concentration (%)	0-4
Average size of nano particles (nm)	5-282

Table 2. Ranges of parameters for Al_2O_3/EG nanofluid

Parameter	Range
Temperature (℃)	10-70
Volumetric concentration (%)	0.25-5
Average size of nanoparticles (nm)	2-53

3.1. Applying GMDH method by using temperature and concentration

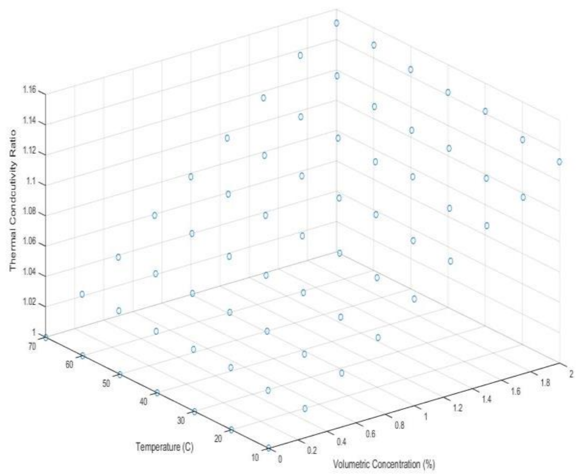

Figure 1. Thermal conductivity ratio vs temperature and concentration for Al_2O_3/water nanofluid [61]

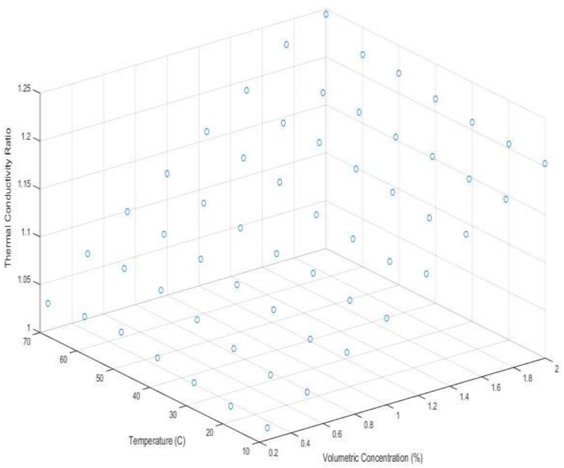

Figure 2. Thermal conductivity ratio vs temperature and concentration for Al_2O_3/EG nanofluid [61]

Based on the literature review, thermal conductivity of nanofluids increase as the temperature or/and concentration increase. Various studied investigated the effect of temperature on thermal conductivity of nanofluids [58-59]. Improvement in thermal conductivity by temperature increase is attributed to the Brownian motion and nano structures' thermophoresis behavior [60]. Moreover, increase in concentration of nano particles increases thermal conductivity due to higher thermal conductivity of solid particles in comparison with the base fluids. Figures 2 & 3 show the results of a study conducted by Agarwal et al. [61] which investigated the effects of temperature and concentration on the thermal conductivity of alumina nano particles in water and EG.

In order to utilize GMDH method for predicting thermal conductivity ratio of the nanofluids, data are extracted from experimental data represented in Refs [61–70]. By applying the GMDH method, thermal conductivity ratio obtained as below:

Thermal Conductivity Ratio = -0.0115572 + N17*0.645631 + N71*0.364922

The calculation procedure of coefficient is represented in appendix 1.

The obtained results by considering temperature and concentration as input variables in GMDH method, are shown in figures 4 to 6 for the water-based nanofluid.

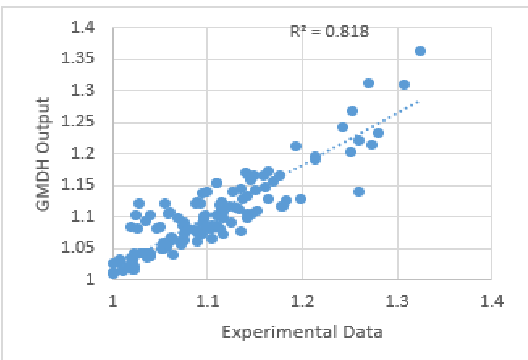

Figure 3. Experimental data vs GMDH output for thermal conductivity ratio of Al_2O_3/water nanofluid

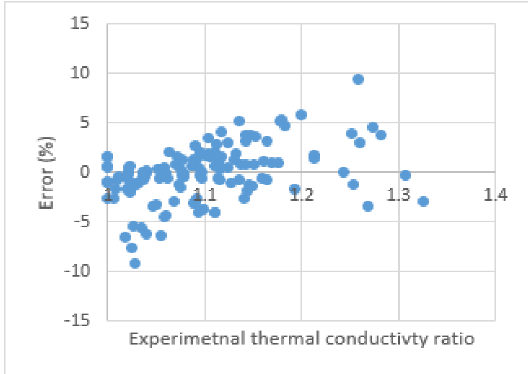

Figure 4. Error for various values of thermal conductivity ratio of Al_2O_3/water nanofluid

Figure 5. Comparison between experimental data and GMDH output for Al_2O_3/water nanofluid

The R-squared and RMSE values for the proposed model by considering temperature and concentration as input variables are 0.818 and 0.0306, respectively. These values show that the proposed model is not appropriate for prediction and the input variables are not adequate.

In addition to water – based nanofluid, thermal conductivity ratio of the Al_2O_3/EG nanofluid is obtained by considering temperature and concentration as input variables.

Obtained results by applying GMDH method are compared with experimental data in figures 7 to 9.

Thermal conductivity ratio = -0.119797 - N196^2*0.0907248 + N6*1.20918

The calculation procedure of coefficient is represented in appendix 2.

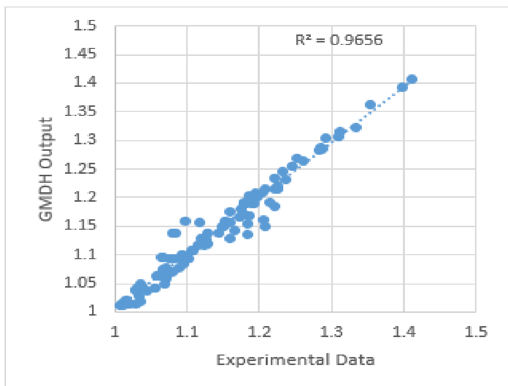

Figure 6. Experimental data vs GMDH output for thermal conductivity ratio of Al_2O_3/EG nanofluid

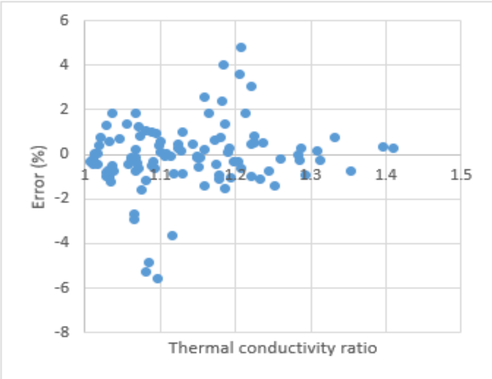

Figure 7. Error for various values of thermal conductivity ratio of Al_2O_3/EG nanofluid

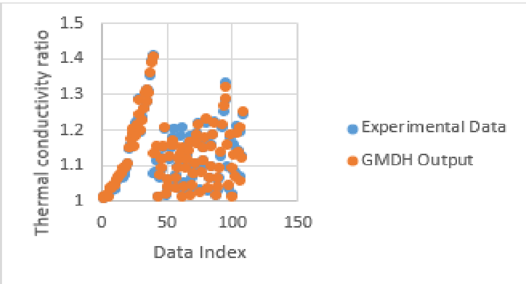

Figure 8. Comparison between experimental data and GMDH output for Al_2O_3/EG nanofluid

The R-squared and RMSE values for the proposed model for Al_2O_3/EG nanofluid are 0.965 and 0.017, respectively.

3.2. Applying GMDH method by using temperature, concentration and size of nanoparticles

In addition to temperature and concentration, the size of nanoparticles is another influential parameter on thermal conductivity. The majority of studies concluded that the increase in particle size leads to enhancement in thermal conductivity; however, there must be an optimal size for nanoparticles and the improvement in thermal conductivity is not unlimited [71].

By considering size, temperature and concentration of nanofluid, the results are obtained more accurately as shown in figures 10 to 12. The obtained regression fit obtained as:

Thermal conductivity ratio = -0.033918 + N189*N2*4.82245 - N189^2*2.41237 + N2*1.05937 - N2^2*2.4346

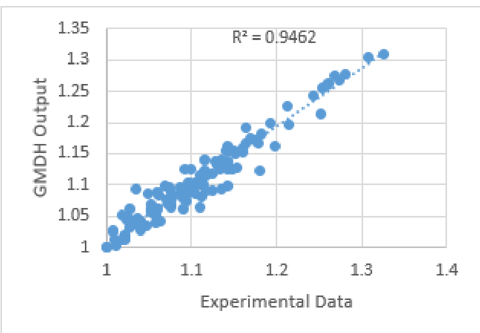

Figure 9. Experimental data vs GMDH output for thermal conductivity ratio of Al_2O_3/water nanofluid

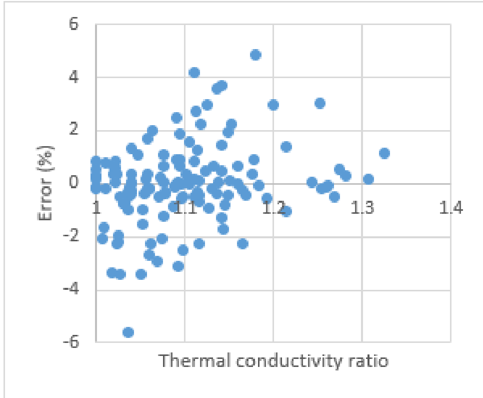

Figure 10. Error for various values of thermal conductivity ratio of Al_2O_3/water nanofluid

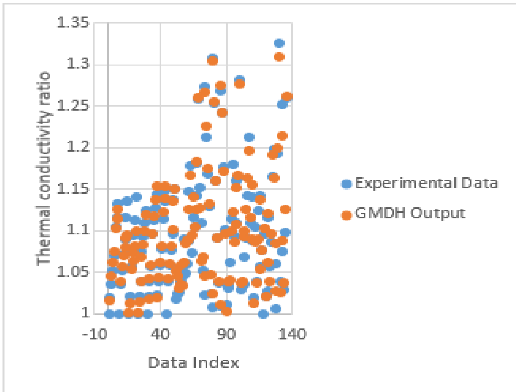

Figure 11. Comparison between experimental data and GMDH output for Al_2O_3/water nanofluid

The calculation procedure of coefficient is represented in appendix 3.

By comparing the results of GMDH output with and without considering particle size, it is concluded that using particle size as one of the input variables leads to obtain more accurate regression. The R-squared and RMSE in this condition are equal to 0.9462 and 0.0166. The maximum error for predicted data by applying GMDH method and considering temperature, size and concentration as input variables is less than 6% which shows the accuracy of the proposed model.

The proposed model by using GMDH approach for Al_2O_3/EG nanofluid by considering three input variables (size, temperature and concentration) obtained as:

Thermal conductivity ratio = -0.000286792 + N12*0.560308 + N23*0.439945

The calculation procedure of coefficient is represented in appendix 3.

Comparison between obtained results by GMDH method and experimental data are and RMSE values are equal to 0.9958 and 0.0059, respectively.

4. CONCLUSION

In this study, GMDH artificial neural network was applied in order to propose a model for thermal conductivity ratio of Al_2O_3/water and Al_2O_3/EG nanofluids. Firstly, temperature and concentration were considered as input variables for the model. Obtained R-square values based on 2-variable model, were 0.818 and 0.965 for Al_2O_3 /water and Al_2O_3 /EG, respectively. Since the size of nanoparticles is an influential parameter on thermal conductivity ratio of nanofluids, particle size added to input variables in the second stage to compare results. Based on obtained results, the R-square values of the proposed models by considering three variables (size, temperature and concentration), were 0.9462 and 0.9958, respectively. Results indicated that the models with three input variables were more precise and applicable.

REFERENCES

[1] Narei H, Ghasempour R, Noorollahi Y. (2016). The effect of employing nanofluid on reducing the bore length of a vertical ground-source heat pump. Energy Convers. Manag. 123: 581-591. https://doi.org/10.1016/j.enconman.2016.06.079

[2] Jiang S, Zhou D, Zhang L, Ouyang J, Yu X, Cui X, Han B. (2018). Comparison of compressive strength and electrical resistivity of cementitious composites with different nano- and micro-fillers. Arch. Civ. Mech. Eng. 18: 60–68. https://doi.org/10.1016/j.acme.2017.05.010

[3] Solanki JN, Murthy ZVP. (2011). Preparation of silver nanofluids with high electrical conductivity preparation of silver nanofluids with high electrical conductivity. Journal of Dispersion Science and Technology 32(5): 724–730. https://doi.org/10.1080/01932691.2010.480863

[4] Mohammadi M, Mohammadi M, Ghahremani AR, Shafii MB, Mohammadi N. (2014). Experimental investigation of thermal resistance of a ferrofluidic closed-loop pulsating heat pipe. Heat Transf. Eng. 35: 25–33. https://doi.org/10.1080/01457632.2013.810086

[5] Gandomkar A, Saidi MH, Shafii MB, Vandadi M, Kalan K. (2017). Visualization and comparative investigations of pulsating ferro-fluid heat pipe. Appl. Therm. Eng. 116: 56–65. https://doi.org/10.1016/j.applthermaleng.2017.01.068

[6] Aybar HŞ, Sharifpur M, Azizian MR, Mehrabi M, Meyer JP. (2015). A review of thermal conductivity models for nanofluids. Heat Transf. Eng. 36: 1085–1110. https://doi.org/10.1080/01457632.2015.987586

[7] Nazari MA, Ghasempour R, Ahmadi MH, Heydarian G, Shafii MB. (2018). Experimental investigation of graphene oxide nanofluid on heat transfer enhancement of pulsating heat pipe. Int. Commun. Heat Mass Transf. 91: 90–94. https://doi.org/10.1016/j.icheatmasstransfer.2017.12.006

[8] Amin TE, Roghayeh G, Fatemeh R, Fatollah P. (2015). Evaluation of nanoparticle shape effect on a nanofluid based flat-plate solar collector efficiency. Energy Explor. Exploit. 33: 659–676. https://doi.org/10.1260/0144-5987.33.5.659

[9] Ali F, Arif M, Khan I, Sheikh NA, Saqib M. (2018) Natural convection in polyethylene glycol based molybdenum disulfide nanofluid with thermal radiation, chemical reaction and ramped wall temperature. Int. J. Heat Technol. 36: 619–631. https://doi.org/10.18280/ijht.360227

[10] Tawfik MM. (2017). Experimental studies of nanofluid thermal conductivity enhancement and applications: A review. Renew. Sustain. Energy Rev. 75: 1239-1253. https://doi.org/10.1016/j.rser.2016.11.111

[11] Ponmani S, William JKM, Samuel R, Nagarajan R, Sangwai JS. (2014). Formation and characterization of thermal and electrical properties of CuO and ZnO nanofluids in xanthan gum, colloids surfaces a physicochem. Eng. Asp. 443: 97-43. https://doi.org/10.1016/j.colsurfa.2013.10.048

[12] Alawi OA, Sidik NAC, Hong WX, Kean TH, Kazi SN. (2018). Thermal conductivity and viscosity models of metallic oxides nanofluids. Int. J. Heat Mass Transf. 116: 1314-1325. https://doi.org/10.1016/J.IJHEATMASSTRANSFER.2017.09.133

[13] Cui W, Shen Z, Yang J, Wu S. (2015). Molecular dynamics simulation on flow behaviors of nanofluids confined in nanochannel. Case Stud. Therm. Eng. 5: 114–121. https://doi.org/10.1016/j.csite.2015.03.007

[14] Hatami M. (2018). Different shapes of Fe_3O_4/nanoparticles on the free convection and entropy generation in a wavy-wall square cavity filled by power-law non-Newtonian nanofluid. Int. J. Heat Technol. 36: 509–524. https://doi.org/10.18280/ijht.360215

[15] Sivakumar A, Alagumurthi N, Senthilvelan T. (2016). Experimental investigation of forced convective heat transfer performance in nanofluids of Al_2O_3/water and CuO/water in a serpentine shaped micro channel heat sink. Heat Mass Transf. Und Stoffuebertragung 52: 1265–1274. https://doi.org/10.1007/s00231-015-1649-5

[16] Akilu S, Baheta AT, Sharma KV, US PT, Mol. Liq. J. (2017). https://doi.org/10.1016/j.molliq.2017.09.017

[17] Shanbedi M, Zeinali Heris S, Amiri A, Baniadam M, Heris S.Z., Amiri A., Baniadam M. (2014). Improvement in heat transfer of a two-phased closed thermosyphon using silver-decorated MWCNT/water. J. Dispers. Sci. Technol. 35(8): 1086-1096. https://doi.org/10.1080/01932691.2013.833101

[18] Kouloulias K, Sergis A, Hardalupas Y, Barrett TR. (2017). Measurement of flow velocity during turbulent natural convection in nanofluids. Fusion Eng. Des. 123: 72-76. https://doi.org/10.1016/J.FUSENGDES.2017.05.120

[19] Bahiraei M. (2014). A comprehensive review on different numerical approaches for simulation in nanofluids: Traditional and novel techniques. J. Dispers. Sci. Technol. 35: 984-996. https://doi.org/10.1080/01932691.2013.825210

[20] Aramesh M, Pourfayaz F, Kasaeian A. (2017). Numerical investigation of the nanofluid effects on the heat extraction process of solar ponds in the transient step. Sol. Energy 157: 869-879. https://doi.org/10.1016/J.SOLENER.2017.09.011

[21] Kahani M, Heris SZ, Mousavi SM. (2013). Effects of curvature ratio and coil pitch spacing on heat transfer performance of Al_2O_3 /water nanofluid laminar flow through helical coils. J. Dispers. Sci. Technol. 34: 1704-1712. https://doi.org/10.1080/01932691.2013.764485

[22] Rashidi S, Farzin F, Amiri A, Shanbedi M. (2015). Heat transfer coefficient prediction of metal oxides based water nanofluids under laminar flow regime using adaptive neuro-fuzzy inference system. Journal of Dispersion Science & Technology 37(9): 1277-2691. https://doi.org/10.1080/01932691.2015.1090318

[23] Taylor P, Tabari ZT, Heris SZ. (2015). Heat transfer

performance of milk pasteurization plate heat exchangers using MWCNT/water nanofluid heat transfer performance of milk pasteurization plate heat exchangers using MWCNT/water nanofluid. Journal of Dispersion Science and Technology 36(2): 37-41. https://doi.org/10.1080/01932691.2014.894917
[24] Salimpour MR, Abdollahi A, Afrand M. (2017). An experimental study on deposited surfaces due to nanofluid pool boiling: Comparison between rough and smooth surfaces. Exp. Therm. Fluid Sci. 88: 288-300. https://doi.org/10.1016/J.EXPTHERMFLUSCI.2017.06.007
[25] Fang X, Chen Y, Zhang H, Chen W, Dong A, Wang R. (2016). Heat transfer and critical heat flux of nanofluid boiling: A comprehensive review. Renew. Sustain. Energy Rev. 62: 924–940. https://doi.org/10.1016/J.RSER.2016.05.047
[26] Minakov AV, Pryazhnikov MI, Guzei DV, Zeer GM, Rudyak VY. (2017). The experimental study of nanofluids boiling crisis on cylindrical heaters. Int. J. Therm. Sci. 116: 214–223. https://doi.org/10.1016/J.IJTHERMALSCI.2017.02.019
[27] Dadjoo M, Etesami N, Esfahany MN. (2017). Influence of orientation and roughness of heater surface on critical heat flux and pool boiling heat transfer coefficient of nanofluid. Appl. Therm. Eng. 124: 353–361. https://doi.org/10.1016/J.APPLTHERMALENG.2017.06.025
[28] Hong TK, Yang HS, Choi CJ. (2005). Study of the enhanced thermal conductivity of Fe nanofluids. J. Appl. Phys. 97(6): 280-441. https://doi.org/10.1063/1.1861145
[29] Garg J, Poudel B, Chiesa M, Gordon JB, Ma JJ, Wang JB, Ren ZF. (2008). Enhanced thermal conductivity and viscosity of copper nanoparticles in ethylene glycol nanofluid Enhanced thermal conductivity and viscosity of copper nanoparticles in ethylene glycol nanofluid. Journal of Applied Physics 103: 074301. https://doi.org/10.1063/1.2902483
[30] Zhang H, Wu Q, Lin J, Chen J, Xu Z, Zhang H, Wu Q, Lin J, Chen J, Xu Z. (2010). Thermal conductivity of polyethylene glycol nanofluids containing carbon coated metal nanoparticles Thermal conductivity of polyethylene glycol nanofluids containing carbon coated metal nanoparticles. Journal of Applied Physics 108(12): 124306. https://doi.org/10.1063/1.3486488
[31] Kannaiyan S, Boobalan C, Umasankaran A, Ravirajan A, Sathyan S, Thomas T. (2017). Comparison of experimental and calculated thermophysical properties of alumina/cupric oxide hybrid nanofluids. J. Mol. Liq. 244. https://doi.org/10.1016/j.molliq.2017.09.035
[32] Taylor P, Yu W, Xie H, Wang X, Yu W, Xie H, Wang X. (2011). Enhanced thermal conductivity of liquid paraffin based nanofluids containing copper nanoparticles. Journal of Dispersion Science & Technology 32(7): 948–951. https://doi.org/10.1080/01932691.2010.488503
[33] Sadri R, Kamali KZ, Hosseini M, Zubir N, Kazi SN, Ahmadi G, Dahari M, Huang NM, Golsheikh AM, Sadri R, Kamali KZ, Hosseini M, Zubir N, Kazi SN. (2017). Experimental study on thermo-physical and rheological properties of stable and green reduced graphene oxide nanofluids : Hydrothermal assisted technique. J. Dispers. Sci. Technol. 38: 1302–1310. https://doi.org/10.1080/01932691.2016.1234387
[34] Pal B, Mallick SS. (2014). Anisotropic CuO nanostructures of different size and shape exhibit thermal conductivity superior than typical bulk powder, colloids surfaces a physicochem. Eng. Asp. 459: 282–289. https://doi.org/10.1016/j.colsurfa.2014.07.017
[35] Sheikholeslami M, Ganji DD. (2017). Numerical modeling of magnetohydrodynamic CuO—Water transportation inside a porous cavity considering shape factor effect, colloids surfaces a physicochem. Eng. Asp. 529: 705–714. https://doi.org/10.1016/j.colsurfa.2017.06.046
[36] Timofeeva EV, Routbort JL, Singh D, Timofeeva EV, Routbort JL, Singh D. (2013). Particle shape effects on thermophysical properties of alumina nanofluids Particle shape effects on thermophysical properties of alumina nanofluids. Journal of Applied Physics 106: 014304. https://doi.org/10.1063/1.3155999
[37] Shaikh S, Lafdi K, Ponnappan R. (2007). Thermal conductivity improvement in carbon nanoparticle doped PAO oil : An experimental study Thermal conductivity improvement in carbon nanoparticle doped PAO oil: An experimental study. Journal of Applied Physics 101(6): 36. https://doi.org/10.1063/1.2710337
[38] Esfe MH, Hajmohammad MH. (2017). Thermal conductivity and viscosity optimization of nanodiamond-Co_3O_4 / EG (40 : 60) aqueous nano fl uid using NSGA-II coupled with RSM. J. Mol. Liq. 238: 545–552. https://doi.org/10.1016/j.molliq.2017.04.056
[39] Taylor P, Kahani M, Heris SZ, Mousavi SM. (2013). Effects of curvature ratio and coil pitch spacing on heat transfer performance of Al_2O_3 / Water nanofluid laminar flow through helical coils effects of curvature ratio and coil pitch spacing on heat transfer. Journal of Dispersion Science and Technology 37–41. https://doi.org/10.1080/01932691.2013.764485
[40] Abdullah AA, Althobaiti SA, Lindsay KA. (2018). Marangoni convection in water–alumina nanofluids: Dependence on the nanoparticle size. Eur. J. Mech. - B/Fluids. 67: 259–268. https://doi.org/10.1016/J.EUROMECHFLU.2017.09.015
[41] Akhavan-Zanjani H, Saffar-Avval M, Mansourkiaei M, Ahadi M, Sharif F. (2014). Turbulent convective heat transfer and pressure drop of graphene–water nanofluid flowing inside a horizontal circular tube. J. Dispers. Sci. Technol. 35: 1230–1240. https://doi.org/10.1080/01932691.2013.834423
[42] Heris SZ, Shokrgozar M, Poorpharhang S, Shanbedi M., Noie SH. (2014). Experimental study of heat transfer of a car radiator with CuO/ethylene glycol-water as a coolant. J. Dispers. Sci. Technol. 35: 677–684. https://doi.org/10.1080/01932691.2013.805301
[43] Mikkola V, Puupponen S, Granbohm H, Saari K, Ala-Nissila T, Seppälä A. (2018). Influence of particle properties on convective heat transfer of nanofluids. Int. J. Therm. Sci. 124: 187–195. https://doi.org/10.1016/j.ijthermalsci.2017.10.015
[44] Hemmat Esfe M, Rostamian H, Reza Sarlak M, Rejvani M, Alirezaie A. (2017). Rheological behavior characteristics of TiO_2-MWCNT/10w40 hybrid nano-oil affected by temperature, concentration and shear rate: An experimental study and a neural network simulating. Phys. E Low-Dimensional Syst. Nanostructures 94: 231–240. https://doi.org/10.1016/J.PHYSE.2017.07.012

[45] Hemmat Esfe M, Hassani Ahangar MR, Rejvani M, Toghraie D, Hajmohammad MH. (2016). Designing an artificial neural network to predict dynamic viscosity of aqueous nanofluid of TiO_2 using experimental data. Int. Commun. Heat Mass Transf. 75: 192–196. https://doi.org/10.1016/J.ICHEATMASSTRANSFER.2016.04.002
[46] Hemmat Esfe M, Bahiraei M, Hajmohammad MH, Afrand M. (2017). Rheological characteristics of MgO/oil nanolubricants: Experimental study and neural network modeling. Int. Commun. Heat Mass Transf. 86: 245–252. https://doi.org/10.1016/J.ICHEATMASSTRANSFER.2017.05.017
[47] Ahmadi Nadooshan A, Hemmat Esfe M, Afrand M. (2017). Prediction of rheological behavior of SiO_2-MWCNTs/10W40 hybrid nanolubricant by designing neural network. J. Therm. Anal. Calorim. 1–8. https://doi.org/10.1007/s10973-017-6688-3
[48] Alirezaie A, Saedodin S, Esfe MH, Rostamian SH. (2017). Investigation of rheological behavior of MWCNT (COOH-functionalized)/MgO - engine oil hybrid nanofluids and modelling the results with artificial neural networks. J. Mol. Liq. 241: 173–181. https://doi.org/10.1016/J.MOLLIQ.2017.05.121
[49] Hemmat Esfe M, Tatar A, Ahangar MRH, Rostamian H. (2018). A comparison of performance of several artificial intelligence methods for predicting the dynamic viscosity of TiO_2/SAE 50 nano-lubricant. Phys. E Low-Dimensional Syst. Nanostructures 96: 85–93. https://doi.org/10.1016/J.PHYSE.2017.08.019
[50] Esfe MH, Esfande S, Rostamian SH. (2017). Experimental evaluation, new correlation proposing and ANN modeling of thermal conductivity of ZnO-DWCNT/EG hybrid nanofluid for internal combustion engines applications. Appl. Therm. Eng. https://doi.org/10.1016/j.applthermaleng.2017.11.131
[51] Hemmat Esfe M, Esfandeh S, Saedodin S, Rostamian H. (2017). Experimental evaluation, sensitivity analyzation and ANN modeling of thermal conductivity of ZnO-MWCNT/EG-water hybrid nanofluid for engineering applications. Appl. Therm. Eng. 125: 673–685. https://doi.org/10.1016/J.APPLTHERMALENG.2017.06.077
[52] Afrand M, Hemmat Esfe M, Abedini E, Teimouri H. (2017). Predicting the effects of magnesium oxide nanoparticles and temperature on the thermal conductivity of water using artificial neural network and experimental data. Phys. E Low-Dimensional Syst. Nanostructures 87: 242–247. https://doi.org/10.1016/j.physe.2016.10.020
[53] Esfe MH, Rejvani M, Karimpour R, Abbasian Arani AA. (2017). Estimation of thermal conductivity of ethylene glycol-based nanofluid with hybrid suspensions of SWCNT–Al_2O_3 nanoparticles by correlation and ANN methods using experimental data. J. Therm. Anal. Calorim. 128: 1359–1371. https://doi.org/10.1007/s10973-016-6002-9
[54] Rostamian SH, Biglari M, Saedodin S, Hemmat Esfe M, (2017). An inspection of thermal conductivity of CuO-SWCNTs hybrid nanofluid versus temperature and concentration using experimental data. ANN modeling and new correlation. J. Mol. Liq. 231: 364–369. https://doi.org/10.1016/J.MOLLIQ.2017.02.015
[55] Kasaeian A, Ghalamchi M, Ahmadi MH, Ghalamchi M. (2017). GMDH algorithm for modeling the outlet temperatures of a solar chimney based on the ambient temperature. Mech. Ind. 18: 216. https://doi.org/10.1051/meca/2016034
[56] Ahmadi MH, Ahmadi MA, Mehrpooya M, Rosen MA. (2015). Using GMDH neural networks to model the power and torque of a stirling engine. Sustain 72243–2255. https://doi.org/10.3390/su7022243
[57] Pourkiaei SM, Ahmadi MH, Hasheminejad SM. (2016). Modeling and experimental verification of a 25W fabricated PEM fuel cell by parametric and GMDH-type neural network. Mech. Ind. 17: 105. https://doi.org/10.1051/meca/2015050
[58] Das PK, Islam N, Santra AK, Ganguly R. (2017). Experimental investigation of thermophysical properties of Al_2O_3–water nanofluid: Role of surfactants, J. Mol. Liq. 237. https://doi.org/10.1016/j.molliq.2017.04.099
[59] Das PK. (2017). A review based on the effect and mechanism of thermal conductivity of normal nanofluids and hybrid nanofluids. J. Mol. Liq. 240. https://doi.org/10.1016/j.molliq.2017.05.071
[60] Ilyas SU, Pendyala R, Narahari M. (2017). Stability and thermal analysis of MWCNT-thermal oil-based nanofluids, colloids surfaces a physicochem. Eng. Asp. 527: 11–22. https://doi.org/10.1016/j.colsurfa.2017.05.004
[61] Agarwal R, Verma K, Agrawal NK, Singh R. (2017). Sensitivity of thermal conductivity for Al_2O_3 nanofluids. Exp. Therm. Fluid Sci. 8019–26. https://doi.org/10.1016/j.expthermflusci.2016.08.007
[62] Senthilraja S, Vijayakumar K, Gangadevi R. (2015). A comparative study on thermal conductivity of Al_2O_3 /water, cuo/water and – cuo/water nanofluids. Dig. J. Nanomater. Biostructures. 10(4): 1449–1458. http://www.chalcogen.ro/1449_Senthilraja.pdf, accessed October 16, 2017.
[63] Hemmat Esfe M, Afrand M, Yan WM, Akbari M. (2015). Applicability of artificial neural network and nonlinear regression to predict thermal conductivity modeling of Al_2O_3–water nanofluids using experimental data. Int. Commun. Heat Mass Transf. 66: 246–249. https://doi.org/10.1016/j.icheatmasstransfer.2015.06.002
[64] Li CH, Peterson GP. (2007). The effect of particle size on the effective thermal conductivity of Al_2O_3-water nanofluids. J. Appl. Phys. 101: 044312. https://doi.org/10.1063/1.2436472
[65] Wang Y, Wu JM. (2015). Numerical simulation on single bubble behavior during Al_2O_3 /H_2O nanofluids flow boiling using moving particle simi-implicit method. Progress in Nuclear Energy 85: 130-139. https://doi.org/10.1016/j.pnucene.2015.06.017
[66] Esfe MH, Saedodin S, Mahian O, Wongwises S. (2014). Thermal conductivity of Al_2O_3/water nanofluids: Measurement, correlation, sensitivity analysis, and comparisons with literature reports. J. Therm. Anal. Calorim. 117: 675–681. https://doi.org/10.1007/s10973-014-3771-x
[67] Li CH, Peterson GP. (2006). Experimental investigation of temperature and volume fraction variations on the effective thermal conductivity of nanoparticle suspensions (nanofluids). J. Appl. Phys. 99: 084314. https://doi.org/10.1063/1.2191571

[68] Lee S, Choi SUS, Li S, Eastman JA. (1999). Measuring thermal conductivity of fluids containing oxide nanoparticles. J. Heat Transfer 121: 280. https://doi.org/10.1115/1.2825978
[69] Beck MP, Yuan Y, Warrier P, Teja AS. (2009). The effect of particle size on the thermal conductivity of alumina nanofluids. J. Nanoparticle Res. 11: 1129–1136. https://doi.org/10.1007/s11051-008-9500-2
[70] Hemmat Esfe M, Karimipour A, Yan WM, Akbari M, Safaei MR, Dahari M. (2015). Experimental study on thermal conductivity of ethylene glycol based nanofluids containing Al_2O_3 nanoparticles. Int. J. Heat Mass Transf. 88: 728–734. https://doi.org/10.1016/j.ijheatmasstransfer.2015.05.010
[71] Pryazhnikov MI, Minakov AV, Rudyak VY, Guzei DV. (2017). Thermal conductivity measurements of nanofluids. Int. J. Heat Mass Transf. 104: 1275–1282. https://doi.org/10.1016/j.ijheatmasstransfer.2016.09.080

APPENDIX 1

*N71 = 1.06079 - N259*2.58978 + N259*N209*0.792102 + N209*1.75108*

*N209 = 5.02276 - N261*3.50572 + N261*N299*4.10165 - N299*4.583*

*N299 = 1.03691 - concentration*0.924928 + concentration*N304*0.871805*

*N261 = 1.04253 - temperature*0.0320422 + temperature*N302*0.030704*

*N259 = 3.48693e-12 + N269*1*

*N17 = -2.4818 - N266*N167*2.05063 + N167*5.51865*

*N167 = 0.407857 + N250*0.211268 + N250*N292*0.379164*

*N292 = 32.9059 - N302*30.4682 + N302*N304*28.6923 - N304*30.0018*

N304 = 1.47349 + temperature*0.0418532 - temperature* $\sqrt[3]{temperature}$ *0.00705606 - $\sqrt[3]{temperature}$ *0.313222

*N250 = 0.0320969 + N269*2.65972 - N279*1.68903*

*N269 = 1.06924 - temperature*0.00119483 + temperature*concentration*0.00169259 - concentration*0.0211386*

*N266 = -2.29609 + N279*2.91761 - N279*N302*1.82553 + N302*2.18258*

N302 = 0.997978 + concentration*0.107522 - concentration* $\sqrt[3]{concentration}$ *0.0429876 + $\sqrt[3]{concentration}$ *0.00726233

N279 = 1.14644 - concentration*0.130648 + concentration* $\sqrt[3]{temperature}$ *0.0518859 - $\sqrt[3]{temperature}$ *0.0363114

Appendix 2

*N6 = 0.131852 + N42^2*0.0983067 + N23*0.77152*

*N23 = -0.493869 + N241*N36*47.0535 - N241^2*23.7864 + N36*1.83383 - N36^2*23.6136*

*N36 = -0.00345911 + N68*0.450018 + N105*0.553037*

*N105 = -0.130651 + N235*1.96563 + N235*N129*110.748 - N235^2*56.3859 - N129*0.759341 - N129^2*54.438*

*N129 = -0.167899 - N192*0.788695 - N192*N221*110.346 + N192^2*55.8412 + N221*2.11734 + N221^2*54.3414*

*N235 = 0.164618 - N300*2.33927 - N300*N323*2.28051 + N300^2*2.40457 + N323*3.05147*

*N300 = 1.21581 - concentration^2*0.00173893 - N319*1.20054 + N319^2*0.994582*

*N68 = 0.587159 - N142*N151*70.1059 + N142^2*35.1058 + N151^2*35.4198*

*N151 = -0.00441004 + N192*0.46583 + N217*0.538064*

*N192 = 0.394507 + N241*0.312121 + N241*N292*0.29795*

*N142 = 0.470252 + N220*14.4813 - N220*N221*249.946 + N220^2*119.131 - N221*14.2949 + N221^2*131.16*

*N221 = 0.180833 + N252*13.4003 - N252*N285*194.021 + N252^2*91.5259 - N285*12.6991 + N285^2*102.613*

*N220 = 0.425837 - concentration*N252*0.0185734 + N252^2*0.574913*

*N252 = 0.347598 - N321*3.31529 - N321*N324*2.89701 + N321^2*3.1634 + N324*3.70363*

N241 = 1.35933 - $\sqrt[3]{temperature}$ *0.534273 + $\sqrt[3]{temperature}$ *N324*0.32958 + $\sqrt[3]{temperature}$ ^2*0.0307514 - N324^2*0.0287977

*N42 = 0.00779353 - N303*0.285346 + N71*1.27846*

*N71 = 0.0793258 - N156*N186*70.8774 + N156^2*35.7131 + N186*0.86692 + N186^2*35.2173*

*N186 = 0.0296152 - N198*N231*128.519 + N198^2*64.6399 + N231*0.969541 + N231^2*63.8781*

*N231 = 0.580762 - N256*N293*172.682 + N256^2*86.8381 + N293^2*86.2675*

*N293 = 0.23575 + N317*0.589705 + N319^2*0.17737*

*N198 = 0.411202 + N236*0.283245 + N236*N292*0.310356*

N292 = 1.98271 + $\sqrt[3]{concentration}$ *0.704065 - $\sqrt[3]{concentration}$ *N318*0.574967 - N318*3.01295 + N318^2*1.95251

*N236 = 0.433692 - temperature*0.0128194 + temperature*N324*0.0112107 + temperature^2*1.65897e-05 + N324*0.597218*

*N156 = -0.00515273 + N210*0.415879 + N217*0.58867*

*N217 = -0.585315 + N285*35.1752 + N285*N298*1092.37 - N285^2*561.779 - N298*33.2139 - N298^2*530.969*

*N285 = 0.577866 + N318*N319*0.429767*

N319 = 1.02129 - temperature*0.00394802 + temperature* $\sqrt[3]{concentration}$ *0.00316982 + temperature^2*2.19221e-05 + $\sqrt[3]{concentration}$ ^2*0.0750819

N318 = 1.4061 + concentration* $\sqrt[3]{temperature}$ *0.032136 - concentration^2*0.00798288 - $\sqrt[3]{temperature}$ *0.250409 + "temperature, cubert"^2*0.0376592

*N210 = 0.577324 + N245*N256*0.430174*

*N256 = 0.158917 - N317*1.03499 - N317*N324*1.19101 + N317^2*1.31551 + N324*1.75224*

*N245 = 91.6158 - N324*15.1293 + N324*N327*14.258 - N327*147.5 + N327^2*58.7891*

N303 = 0.00176952 - $\sqrt[3]{temperature}$ *0.000716792 + N317*1.00052

*N317 = 1.04749 - temperature*0.00242951 + temperature*concentration*0.001107 + temperature^2*2.61671e-05 + concentration*0.0634356 - concentration^2*0.00771838*

*N196 = 0.0184285 + N228*2.17991 + N228*N237*36.871 - N228^2*19.2842 - N237*1.20936 - N237^2*17.5734*

*N237 = -0.807522 - N298*23.7389 + N298*N320*435.333 - N298^2*207.154 + N320*26.1194 - N320^2*228.759*

*N320 = 93.1798 - concentration*1.45848 + concentration*N327*1.3814 - concentration^2*0.00801795 - N327*162.726 + N327^2*71.807*

N327 = 1.0571 + $\sqrt[3]{temperature}$ *0.0229108

*N298 = 1.11674 - concentration^2*0.00218232 - N321*1.04842 + N321^2*0.939285*

*N228 = -0.00598277 - N262*1.266 + N262^2*0.846248 + N323*2.26972 - N323^2*0.845127*

N323 = -1.2883e-09 + N324*1

N324 = 0.230562 + concentration*11.0776 - concentration* $\sqrt[3]{concentration}$ *4.45051 + concentration^2*0.287269 + $\sqrt[3]{concentration}$ *4.72214 - "concentration, cubert"^2*10.763

N262 = 4.13478 + $\sqrt[3]{concentration}$ *1.3448 - $\sqrt[3]{concentration}$ *N321*1.13784 - N321*7.38699 + N321^2*4.13226

N321 = 1.52002 - $\sqrt[3]{temperature}$ *0.304285 + $\sqrt[3]{temperature}$ * $\sqrt[3]{concentration}$ *0.0955142 + $\sqrt[3]{temperature}$^2*0.0370877 - $\sqrt[3]{concentration}$ *0.233051 + $\sqrt[3]{concentration}$^2*0.0914517

Appendix 3

N2 = -0.0439599 + $\sqrt[3]{temperature}$ *0.0315586 – ($\sqrt[3]{temperature}$)^2*0.00587683 + N3*1.00435

N3 = 0.155496 + N124*3.36364 + N124*N4*10.6424 - N124^2*6.80354 - N4*2.66387 - N4^2*3.69322

N4 = 0.2407 + N133*0.592437 - N133*N6*11.8329 + N133^2*5.52278 + N6^2*6.47899

N6 = 0.172566 - N105*2.66192 + N105*N10*6.1354 - N105^2*1.84191 + N10*3.33287 - N10^2*4.13622

N10 = 0.0168257 - N23*1.5894 - N23*N18*209.588 + N23^2*105.046 + N18*2.57135 + N18^2*104.542

N18 = -2.02643 - " $\sqrt[3]{concentration}$ "*0.895731 + $\sqrt[3]{concentration}$ *N20*0.954151 - ($\sqrt[3]{concentration}$)^2*0.0674471 + N20*5.58932 - N20^2*2.56794

N20 = -0.0169248 + N39*0.569435 + N64*0.44602

N39 = -0.539089 - N232*N71*0.472651 + N71*2.01153

N232 = 1.94648 + N247*33.6372 - N247*N248*28.0279 - N248*36.0753 + N248^2*29.5401

N248 = 0.557289 - N264*N270*11.8467 + N264^2*6.17808 + N270^2*6.11286

N247 = 0.549857 - N272*N264*12.3273 + N272^2*6.35166 + N264^2*6.42436

N23 = -0.014425 + N36*0.593471 + N64*0.4197

N64 = -0.0937814 + N79*1.15177 + N79*N122*85.318 - N79^2*42.6294 - N122^2*42.7439

N122 = 0.548532 + N261*N146*49.3484 - N261^2*24.8914 - N146^2*23.9979

N146 = -0.23137 - N182*N203*0.7618 + N182^2*0.61223 + N203*1.37537

N203 = 2.09602 + N272*3.52473 + N272*N224*35.0648 - N272^2*19.1706 - N224*6.42145 - N224^2*14.0823

N261 = -0.710208 + $\sqrt[3]{size}$ *0.233925 - $\sqrt[3]{size}$ * N270*0.224983 + ($\sqrt[3]{size}$)^2*0.00254334 + N270*1.65562

N79 = -0.0347346 + N102*0.62386 + N139*0.407856

N102 = 0.542353 + N273*N163*28.7982 - N273^2*14.7338 - N163^2*13.5996

N163 = 0.217553 - N224*N260*7.71021 + N224^2*4.12828 + N260*0.60079 + N260^2*3.76162

N36 = -0.591883 - N216*N71*0.517506 + N71*2.10902

N71 = 0.551944 - N119*N139*11.075 + N119^2*5.74133 + N139^2*5.7826

N139 = 1.55236 - N272*1.90194 + N272*N166*30.9343 - N272^2*14.9265 - N166^2*14.6503

N166 = -8.82794 + N276*19.9028 + N276*N254*6.69713 - N276^2*12.0441 - N254*3.55413 - N254^2*1.29918

N254 = 27.6859 + $\sqrt[3]{concentration}$ *6.98392 - $\sqrt[3]{concentration}$ *N272*7.25464 + ($\sqrt[3]{concentration}$)^2*0.412021 - N272*56.9199 + N272^2*30.2604

N119 = 0.851494 + N182*11.6096 - N182*N188*105.899 + N182^2*47.6807 - N188*12.1472 + N188^2*58.9018

N188 = 1.42085 - $\sqrt[3]{temperature}$ * 0.588204 + $\sqrt[3]{temperature}$ *N260*0.467063 + ($\sqrt[3]{temperature}$)^2*0.0172111 - N260^2*0.21691

N182 = 29.0248 + $\sqrt[3]{concentration}$ *8.76141 - $\sqrt[3]{concentration}$ * N270*9.09928 + ($\sqrt[3]{concentration}$)^2*0.521972 - N270*61.0681 + N270^2*33.0526

N216 = 0.546654 + N251*N255*0.481086 - N255*0.0274444

N255 = 0.289361 - $\sqrt[3]{temperature}$ *0.371995 + $\sqrt[3]{temperature}$ *N264*0.246878 + ($\sqrt[3]{temperature}$)^2*0.0194641 + N264*1.46935 - N264^2*0.567788

N251 = 1.05743 - $\sqrt[3]{temperature}$ *0.332809 + $\sqrt[3]{temperature}$ *N270*0.314313

N105 = -0.0935853 + N154*N249*105.233 - N154^2*51.5875 + N249*1.18871 - N249^2*53.7343

N249 = 0.556159 - N265*N269*10.2422 + N265^2*5.3785 + N269^2*5.30922

N269 = 0.5535 + N270^2*0.450366

N270 = 1.79649 - N272*N274*12.909 + N272^2*6.75012 - N274*2.30547 + N274^2*7.67239

N265 = 8.05927 - N276*8.19174 + N276*N273*7.9282 - N273*5.8934 - N273^2*0.87347

N154 = 0.042493 + N198*0.938548 - N198*N244*27.173 + N198^2*13.4947 + N244^2*13.6932

N244 = 0.658433 + N260*2.99416 - N260*N264*2.12405 - N264*3.20345 + N264^2*2.67723

N264 = 8.29568 - N274*6.43445 + N274*N276*7.84398 - N274^2*0.586885 - N276*8.08886

N198 = 1.96822 + N276*6.0685 + N276*N262*9.18779 - N276^2*7.08292 - N262*9.1697

N262 = 1.21061 - $\sqrt[3]{temperature}$ *0.432062 + $\sqrt[3]{temperature}$ *N272*0.326664 + ($\sqrt[3]{temperature}$)^2*0.011487

N133 = 0.533045 + N271*N147*14.0159 - N271^2*7.13996 - N147^2*6.40515

N147 = 0.453799 - N204*2.8159 - N204*N212*61.038 + N204^2*32.0004 + N212*3.04547 + N212^2*29.353

N212 = 1.21768 + N258^2*0.258996 - N260*1.25115 + N260^2*0.778276

N258 = 3.26009 - $\sqrt[3]{concentration}$ *2.51817 + $\sqrt[3]{concentration}$ *N276*2.41249 - N276*2.10711

N204 = 0.568517 + N224*6.03238 - N224*N256*4.76589 - N256*6.1257 + N256^2*5.28845

N224 = 13.3683 - N272*13.3582 + N272*N276*14.1144 - N272^2*0.530601 - N276*10.3193 - N276^2*2.19885

N276 = 0.355487 + $\sqrt[3]{temperature}$ *0.31429 - $\sqrt[3]{temperature}$ * $\sqrt[3]{size}$ * 0.0486913 - ($\sqrt[3]{temperature}$)^2*0.0199388 + $\sqrt[3]{size}$ *0.125759 + ($\sqrt[3]{size}$)^2*0.00316425

N271 = -478.911 + N274*53.3607 - N274*N273*6916.64 + N274^2*3042.39 + N273*819.436 + N273^2*3478.51

N124 = -0.517161 + N273*9.81491 + N273*N191*56.0058 - N273^2*32.7723 - N191*7.89626 - N191^2*23.6331

N191 = 1.12128 - N256*3.66051 - N256*N260*1.89471 + N256^2*2.86522 + N260*2.56987

N260 = 52.004 + $\sqrt[3]{concentration}$ *15.6875 - $\sqrt[3]{concentration}$ *N274*16.3572 + ($\sqrt[3]{concentration}$)^2*1.04945 - N274*109.218 + N274^2*58.2556

N256 = 1.84353 - $\sqrt[3]{temperature}$ *0.864108 + $\sqrt[3]{temperature}$ *N274*0.735576 + ($\sqrt[3]{temperature}$)^2*0.0157507 - N274^2*0.603494

$N273 = 0.549413 + N274^2*0.453859$

Appendix 4

$N23 = 0.00307904 - N277*0.305848 + N28*1.30313$

$N28 = -0.0226528 + N70*N91*8.4779 - N70^2*3.99666 + N91*1.03745 - N91^2*4.49637$

$N91 = 0.0522123 + N125*4.7784 + N125*N212*3.597 - N125^2*3.55704 - N212*3.86989$

$N212 = 0.177446 - N253*6.1007 + N253^2*3.25318 + N387*6.80485 - N387^2*3.13152$

$N387 = 0.141524 - N444*3.39422 - N444*N459*3.10179 + N444^2*3.20254 + N459*4.15331$

$N459 = -124.77 + \sqrt[3]{concentration}*0.0378238 + \sqrt[3]{concentration}^2*0.116687 + N491*222.531 - N491^2*98.4561$

$N444 = -16.3901 + N460*N484*0.877107 + N484*29.7593 - N484^2*13.4876$

$N460 = 1.04749 - temperature*0.00242951 + temperature*concentration*0.001107 + temperature^2*2.61671e-05 + concentration*0.0634356 - concentration^2*0.00771838$

$N253 = 0.314215 + N336*3.73675 - N336*N410*23.1994 + N336^2*10.372 - N410*3.2753 + N410^2*13.0539$

$N410 = -91.7218 - N462*N491*0.63044 + N462^2*0.758592 + N491*163.368 - N491^2*71.9743$

$N491 = 1.47363 - \sqrt[3]{size}*0.268828 + \sqrt[3]{size}^2*0.0464843$

$N462 = 1.02129 - temperature*0.00394802 + temperature*\sqrt[3]{concentration}*0.00316982 + temperature^2*2.19221e-05 + \sqrt[3]{concentration}^2*0.0750819$

$N125 = 0.0593708 - \sqrt[3]{temperature}*0.0526818 + \sqrt[3]{temperature}^2*0.0103755 + N249*0.999156$

$N249 = 0.210198 - N340*3.14759 - N340*N467*15.9214 + N340^2*9.94396 + N467*3.79125 + N467^2*6.12431$

$N340 = 5.7487 - N431*3.66406 + N431*N485*5.85338 - N431^2*0.874882 - N485*6.0452$

$N70 = -0.151182 - N436*1.75082 + N436*N132*1.09555 + N132*3.01942 - N132^2*1.21378$

$N132 = 0.111289 + N473*2.68781 - N473*N311*15.0922 + N473^2*6.13742 - N311*1.84972 + N311^2*9.00755$

$N311 = 5.25361 - N422*3.29345 + N422*N478*5.52594 - N422^2*0.875062 - N478*5.60742$

$N478 = 2.54991e-11 + N489*1$

$N422 = -0.104214 + N436*4.42879 - N436*N475*3.00016 - N475*3.25346 + N475^2*2.92684$

$N473 = 1.95189 - \sqrt[3]{concentration}*2.21891 + \sqrt[3]{concentration}*N485*2.18895 - N485^2*0.859319$

$N12 = -0.122877 - N368^2*0.0946185 + N52*1.21636$

$N52 = -0.00143798 + N67*0.602684 + N99*0.398585$

$N99 = -0.0608305 + N379*5.19705 + N379*N141*30.2437 - N379^2*17.5259 - N141*4.08064 - N141^2*12.7719$

$N141 = 0.023142 - N277*7.53984 - N277*N283*101.533 + N277^2*54.1334 + N283*8.50377 + N283^2*47.4106$

$N283 = -0.0661891 - N345*4.98658 - N345*N355*26.189 + N345^2*15.4951 + N355*6.11953 + N355^2*10.6263$

$N355 = 0.320408 - temperature*0.00863531 + temperature*N431*0.00842796 + N431*0.686808$

$N431 = 1.74582 + concentration*0.0621551 + concentration*\sqrt[3]{size}*0.0145533 - concentration^2*0.00384072 - \sqrt[3]{size}*0.636001 + - \sqrt[3]{size}^2*0.116188$

$N345 = 5.68121 - N432*3.72705 + N432*N485*5.67002 - N432^2*0.758563 - N485*5.84749$

$N277 = 0.254285 - N347*1.16728 - N347*N471*19.5149 + N347^2*10.9315 + N471*1.74658 + N471^2*8.75207$

$N471 = 1.97737 - \sqrt[3]{concentration}*2.28187 + \sqrt[3]{concentration}*N489*2.24388 - N489^2*0.878485$

$N347 = 5.86356 - N432*3.85011 + N432*N489*5.85103 - N432^2*0.795616 - N489*6.04829$

$N489 = 1.07598 + temperature*0.0025498 - temperature*size*4.08789e-05 - size*0.00298495 + size^2*6.64561e-05$

$N465 = 1.52002 - \sqrt[3]{temperature}*0.304285 + \sqrt[3]{temperature}*\sqrt[3]{concentration}*0.0955142 + \sqrt[3]{temperature}^2*0.0370877 - \sqrt[3]{concentration}*0.233051 + \sqrt[3]{concentration}^2*0.0914517$

$N282 = 0.0742453 + N342*4.14822 - N342*N428*2.86202 - N428*3.28937 + N428^2*2.92798$

$N493 = 1.0571 + \sqrt[3]{temperature}*0.0229108$

$N428 = 0.433692 - temperature*0.0128194 + temperature*N475*0.0112107 + temperature^2*1.65897e-05 + N475*0.597218$

$N342 = 5.96116 - N436*3.81995 + N436*N484*6.04972 - N436^2*0.904905 - N484*6.26513$

$N169 = 0.501787 - concentration^2*0.0026461 + N282^2*0.497111$

$N475 = 0.230562 + concentration*11.0776 - concentration*\sqrt[3]{concentration}*4.45051 + concentration^2*0.287269 + \sqrt[3]{concentration}*4.72214 - \sqrt[3]{concentration}^2*10.763$

$N67 = -0.0966324 + N120*5.34773 + N120*N169*3.91114 - N120^2*3.97676 - N169*4.18742$

$N379 = 0.0576154 + N432*6.46599 - N432^2*2.52785 - N465*5.58326 + N465^2*2.58636$

$N484 = 0.896649 - size*\sqrt[3]{temperature}*0.0013362 + size^2*6.55798e-05 + \sqrt[3]{temperature}*0.0825952$

$N120 = 25.9835 - N492*45.579 + N492*N250*0.880739 + N492^2*19.9874$

$N250 = 0.201532 - N336*3.01893 - N336*N467*15.9805 + N336^2*9.90949 + N467*3.67825 + N467^2*6.21086$

$N467 = -19.8242 - concentration*0.554298 + concentration*N488*0.590246 - concentration^2*0.0116462 + N488*37.0513 - N488^2*16.4755$

$N488 = 1.1946 + temperature*0.00396623 - temperature*\sqrt[3]{size}*0.000954049 - \sqrt[3]{size}*0.121022 + \sqrt[3]{size}^2*0.0258324$

$N336 = 5.71918 - N436*3.63394 + N436*N485*5.84165 - N436^2*0.882014 - N485*6.02784$

$N485 = 0.836083 + \sqrt[3]{temperature}*0.135803 - \sqrt[3]{temperature}*\sqrt[3]{size}*0.0330707 + \sqrt[3]{size}^2*0.0173862$

$N436 = 1.0698 + concentration*0.0830254 + concentration*size*0.000639263 - concentration^2*0.00367463 - size*0.015615 + size^2*0.000268299$

$N492 = 0.538778 + \sqrt[3]{temperature}*0.0116771 + N493*0.490323$

$N368 = 0.961219 - \sqrt[3]{temperature}*0.33494 + \sqrt[3]{temperature}*N432*0.249184 + \sqrt[3]{temperature}^2*0.0125925 + N432*0.181389$

(1) $N432 = 1.09013 - size*0.0161022 + size*\sqrt[3]{concentration}*0.00166551 + size^2*0.000260082 - \sqrt[3]{concentration}*0.115233 + \sqrt[3]{concentration}*0.173351$